SLAC–PUB–5327 Rev
March 1991
(A/T)

Close Approximations to Invariant Tori in Nonlinear Mechanics*

Robert L. Warnock

Stanford Linear Accelerator Center
Stanford University, Stanford, California 94309

Abstract

A general method to compute precise approximations to invariant tori of Hamiltonian systems is presented. For illustration, a strongly nonlinear example from accelerator theory is treated, in $2\frac{1}{2}$ degrees of freedom. Accuracy, computation time, and effectiveness near resonances are found to be highly favorable in comparison to previous methods.

PACS numbers: 05.45.+6

* Work supported by Department of Energy contract DE–AC03–76SF00515.

The Kolmogorov-Arnol'd-Moser Theorem[1] ensures the existence of toroidal surfaces in phase space that are invariant under the time evolution of a nearly integrable Hamiltonian system. The computation of approximations to these invariant tori is an important topic in several fields of research, including plasma physics,[2] semiclassical quantum theory,[3] celestial mechanics,[4] and accelerator theory.[5] The problem has been treated by various forms of perturbation theory for over a hundred years.[6] Modern formulations of the perturbative method, realized on computers, allow one to carry the perturbation series to rather high orders.[7,8] Nonperturbative numerical methods have also received attention, notably direct solution of the Hamilton-Jacobi equation[9,10] by a projection-iteration method, and methods that depend on fitting of surfaces to orbits.[2,3,4]

This paper describes a method that allows an unprecedented degree of accuracy in relatively little computation time, in examples studied to date. It proceeds by fitting tori to orbit points, using a new and very simple technique to accomplish the fit. It is able to handle large perturbations of integrable systems and find tori very close to resonances, and is therefore more robust than perturbative and nonperturbative schemes that are sensitive to small divisors. It is applicable in principle to any Hamiltonian system. Being based solely on computation of orbits, the method provides a new view of the canonical formalism that proves to have considerable heuristic value. It gives a clearer picture of the effects of resonances, and a better quantification of those effects. On the other hand, all quantities of interest in the traditional formalism can be obtained as well in this scheme; for example, solutions of the Hamilton-Jacobi equation and the corresponding invariant actions.[11]

A reason for studying nearly invariant tori is that a family of such defines a canonical transformation to new action-angle variables such that the action is nearly constant. By studying the residual time variation of the new action one can set bounds on the motion for finite but very long times, as is done in Nekhoroshev's Theorem.[11,12] To obtain stability times of useful magnitude for the study and design of real systems such as particle accelerators, the transformation must be constructed

from very precise approximations to invariant tori, often under conditions of strong nonlinearity. This is a principal motivation for the present work, but our technique also seems promising for cases in which the inclusion of several degrees of freedom is a more urgent matter than high precision.

It is convenient to describe the tori in terms of the action-angle variables $(\mathbf{I}, \mathbf{\Phi})$ of an underlying integrable system. The Hamiltonian will have the form

$$H(\mathbf{I}, \mathbf{\Phi}, \theta) = H_o(\mathbf{I}) + V(\mathbf{I}, \mathbf{\Phi}, \theta) \quad , \tag{1}$$

where H_o describes an integrable system, and the perturbation V is 2π-periodic in $\mathbf{\Phi}$ and θ. The time-like independent variable of Hamilton's equations is θ. In the case of a cyclic accelerator, it represents azimuthal position along a closed reference orbit. Bold faced quantities are vectors of dimension d, the number of mechanical degrees of freedom.

Invariant surfaces arise through a canonical transformation to new action-angle coordinates $(\mathbf{J}, \mathbf{\Psi})$, induced by a generating function $S(\mathbf{J}, \mathbf{\Phi}, \theta) = \mathbf{J} \cdot \mathbf{\Phi} + G(\mathbf{J}, \mathbf{\Phi}, \theta)$ that is 2π-periodic in $\mathbf{\Phi}$ and θ. The relations between old and new coordinates are

$$\mathbf{I} = \mathbf{J} + G_{\mathbf{\Phi}}(\mathbf{J}, \mathbf{\Phi}, \theta) \ , \quad \mathbf{\Psi} = \mathbf{\Phi} + G_{\mathbf{J}}(\mathbf{J}, \mathbf{\Phi}, \theta) \quad , \tag{2}$$

where subscripts denote partial derivatives. If the transformation is ideal, so that $\mathbf{J}$ is invariant, the first equation of (2) defines an invariant torus $\mathbf{I}(\mathbf{\Phi}, \theta)$ of dimension $d+1$. A section of this surface at fixed θ, a torus of dimension d, will be the object of interest. If the system is autonomous, both V and G are independent of θ, the torus has dimension d, and one studies the $(d-1)$-dimensional section obtained by fixing one component of $\mathbf{\Phi}$. Our discussion is easily modified to handle that case.

It is sufficient to study only the points in phase space where orbits intersect a Poincaré surface of section, say the surface defined by $\theta = 0 \pmod{2\pi}$. Our entire discussion is based on the return map $\mathcal{M} : (\mathbf{I}, \mathbf{\Phi})|_{\theta=2\pi n} \mapsto (\mathbf{I}, \mathbf{\Phi})|_{\theta=2\pi(n+1)}$; this corresponds to one turn around an accelerator. Symplectic numerical integration of Hamilton's equations provides a way to evaluate $\mathcal{M}$ for any system of a wide class.[13]

A d-dimensional torus, nearly invariant under $\mathcal{M}$, will be represented as a truncated Fourier series,

$$\mathbf{I} = \mathbf{J} + \mathbf{u}(\mathbf{\Phi}) = \sum_{|m_j| \le M_j} \mathbf{I_m} e^{i\mathbf{m}\cdot\mathbf{\Phi}} \quad , \tag{3}$$

where the components of $\mathbf{m}$ are denoted by m_j. Here $\mathbf{J} = \mathbf{I_o}$ is the constant term of the Fourier series, the average of $\mathbf{I}$ over $\mathbf{\Phi}$; it approximates the invariant action. We seek to determine the Fourier coefficients $\mathbf{I_m}$ so that the torus passes exactly through a finite set of points $(\mathbf{I}(\theta), \mathbf{\Phi}(\theta))$ on a single orbit of $\mathcal{M}$. If the set of points is sufficiently large, we can hope that all additional points on the orbit will be very close to the torus.

To fit the surface (3) to orbit points, one cannot simply take a discrete Fourier transform of $\mathbf{I}(\mathbf{\Phi})$ to obtain the coefficients $\mathbf{I_m}$, because the values of $\mathbf{\Phi}$ on the orbit of $\mathcal{M}$ are scattered unpredictably. One might try instead to solve directly a system of linear equations for the coefficients, but the matrix of this system is dense, of order 1, and too large to be tractable in the cases of greatest interest. To avoid these difficulties we replace the equations for the coefficients by equations for the values of $\mathbf{I}(\mathbf{\Phi})$ on the points of a regular mesh in $\mathbf{\Phi}$.

The scheme will be stated for $d = 1$, since it is essentially the same in any dimension. The discrete Fourier transform of a function $I(\Phi)$ is

$$\hat{I}_m = \frac{1}{K} \sum_{k=0}^{K-1} I(\frac{2\pi k}{K}) \exp(\frac{2\pi i m k}{K}) \quad , \tag{4}$$

which provides an approximation to the Fourier coefficient for $|m| \le M$ when $K = 2M + 1$. Substitute this expression for I_m in (3), then evaluate the sum over m as a geometric series, summing to $|m| = M$ with $K = 2M + 1$. This leads to equations for the $I(2\pi k/K)$:

$$I(\Phi_j) = \sum_{k=0}^{K-1} D_{jk}\, I(\frac{2\pi k}{K}) \, , \qquad D_{jk} = \frac{\sin(\pi(x_j - k))}{K \sin(\pi(x_j - k)/K)} \quad , \tag{5}$$

where $j = 0, 1, \cdots, K-1$ and $\Phi_j = 2\pi x_j / K$. The $(I(\Phi_j), \Phi_j)$ are points on a single orbit of $\mathcal{M}$.

Notice that the matrix D_{jk} of the system (5) tends to δ_{jk} when x_j approaches j for all j. Then if $x_j \approx j$ for all j, the matrix will be close to the unit matrix and the system can be solved by iteration, a process that is feasible for large systems if the number of iterations required is much less than the dimension of the matrix. If the orbit truly lies on an invariant torus, one will find at least one x_j close to every j if the orbit is followed for a sufficiently long time. We obtain a system amenable to iteration by electing to fit the surface just to a subset of points on the orbit, a subset having one and only one x_j close to each j. Convergence of an iterative solution of Eq. (5) is controlled by a parameter r such that $|x_j - j| \leq r$. In examples treated to date, $r = 0.5$ has always ensured convergence. That is, it is sufficient to have one orbit point in each cell of the Φ mesh, anywhere within the cell.

In the case of a low order resonance the method fails, as it should, since it is not possible to find an x_j close to every j; the values of $\mathbf{\Phi}$ on a resonant orbit do not approach every value. This is illustrated in Figure 1 for the example treated below, a case with $d = 2$. Values of $\mathbf{\Phi} = (\Phi_1, \Phi_2)$ are plotted for a resonant orbit corresponding to winding numbers (ν_1, ν_2) such that $7\nu_1 + \nu_2$ is an integer. Figure 2 is a similar plot for an apparent nonresonant orbit. The points fill the plane more and more densely as the orbit is extended. (Of course, in a numerical calculation it is not possible to distinguish a resonance of extremely high order from an invariant torus.) The method succeeds for nonresonant orbits very close to resonant orbits, although it may take more map evaluations than usual to find suitable orbit points.

To illustrate we treat a basic problem of accelerator theory, two-dimensional oscillations transverse to the beam direction ("betatron oscillations") in a cyclic machine.[5] The coordinates $x_i (i = 1, 2)$ are transverse displacements from a closed reference orbit, and the conjugate (dimensionless) momenta are $p_i = dx_i/d(R\theta)$, where $2\pi R$ is the circumference of the reference orbit. The motion is perturbed harmonic motion, with the nonlinear perturbation coming from sextupole magnets that are used to compensate the momentum dependence of the focusing. The field of a sextupole gives a term proportional to $x_1^3 - 3x_1x_2^2$ in the perturbation V. After a transformation to

action-angle variables $(\mathbf{I}, \mathbf{\Phi})$, analogous to the familiar transformation for harmonic oscillators but slightly more involved,[5] the Hamiltonian with n sextupoles takes the form

$$H(\mathbf{I}, \mathbf{\Phi}, \theta) = \boldsymbol{\nu} \cdot \mathbf{I} + \sum_{j=1}^{n} F_j(\theta) \left[(\beta_{1j} I_1)^{3/2} \cos^3(\Phi_1 + \xi_{1j}) \right. \\ \left. -3(\beta_{1j} I_1)^{1/2} \cos(\Phi_1 + \xi_{1j}) \cdot \beta_{2j} I_2 \cos^2(\Phi_2 + \xi_{2j}) \right] \quad . \tag{6}$$

The tunes (winding numbers) ν_i are the unperturbed frequencies normalized to the revolution frequency of the beam. The function $F_j(\theta)$ is nonzero only over the extent of the $j-$th sextupole, where it has a constant value. The constants β_{ij} and ξ_{ij} are determined entirely by linear aspects of the magnets that guide and focus the beam. The action I_i is measured in units of length; it is the usual action divided by the momentum of the beam. The contribution of one sextupole to the time evolution map resembles a two-dimensional quadratic map, since the functions $F_i(\theta)$ are sharply localized and simulate delta functions. Between sextupoles there is linear propagation at constant $\mathbf{I}$.

The reader may notice a certain resemblance of Eq.(6) to the Hénon-Heiles Hamiltonian,[14] but the two examples differ essentially regarding subtle effects of long-term behavior, since the θ-dependence of our perturbation effectively adds one dimension to phase space. Invariant tori permanently confine orbits in the 4-dimensional phase space of Hénon-Heiles, but not in our 5-dimensional space. Our interest is in phenomena like Arnol'd Diffusion that can occur in the larger space.[11] Our method could also be used to study break-up of tori in the Hénon-Heiles model, along the lines of Ref.9 .

We treat a case with four sextupoles, derived from one cell of the magnet configuration for the Berkeley Advanced Light Source. The parameters of Eq. (6) are given in Ref. 10 . The map $\mathcal{M}$ is evaluated through numerical integration of Hamilton's equations by Ruth's fourth order symplectic integrator.[13]

The amount of nonlinearity on an orbit increases with the initial action $\mathbf{I}(\theta = 0)$. We give results for various $\mathbf{I}(0)$, each for $\mathbf{\Phi}(0) = 0$, in a region of substantial

nonlinearity. Figure 3 shows typical orbit data. One action, I_1, is plotted versus the two angles. For linear motion the points would lie in a plane, I_1 =constant. As a measure of the degree of nonlinearity we use the "fluctuation", $f_i = \max_{\mathbf{\Phi}} |I_i(\mathbf{\Phi}) - J_i|/J_i$. We consider fluctuations up to 30%, which are large by the standards of accelerator operation.

We fit surfaces with various maximum mode numbers $M = M_1 = M_2$, finding as expected that more modes (hence more orbit points) are required for good accuracy when $\mathbf{I}(0)$ is large. Eqs. (5) were solved by Gauss-Seidel iteration. The parameter r was taken to be 0.3, which gave sufficient convergence of the iteration in 10 to 15 steps. When a resonance is encountered, the computer code automatically tries a new initial condition.

To test invariance of a torus we compute 100 different orbits $(\hat{\mathbf{I}}(\theta), \hat{\mathbf{\Phi}}(\theta))$ starting at randomly chosen points on the torus, and follow each for 1000 turns. We then examine the deviation of each orbit from the torus $\mathbf{I}(\mathbf{\Phi})$ at the last turn; namely, $d\mathbf{I} = \hat{\mathbf{I}}(\theta) - \mathbf{I}(\hat{\mathbf{\Phi}}(\theta))$ at $\theta = 1000(2\pi)$. Table 1 shows the maximum, over the ensemble of 100 orbits, of the relative deviation $|dI_i|/J_i$. The ensemble average $\langle dI_i \rangle / J_i$ (algebraic average including sign) is also shown.

For 1000 turns the tori are invariant to high accuracy – better than 2 parts in 10^9 at 10% fluctuation, and 2 parts in 10^5 at 30% fluctuation, with $M = 30$. Moreover, the ensemble average of deviations is much less than the maximum deviation, which suggests that the orbits oscillate rather symmetrically about the surfaces.

To evaluate this approach in a context of traditional methods, a comparison to high-order perturbation theory is useful. Results for this example by the method of Ref. 8 , kindly provided by Dr. Forest, are comparable in accuracy to ours for $M = 10$ when the normal-form series is carried to 10-th order. The accuracy that we obtain with $M \geq 20$ is difficult to achieve in reasonable time by the perturbation expansion. A 20-th order expansion took about one hour on the Cray 2, and gave poorer accuracy than our $M = 20$ runs by factors of 3 to 40, depending on $\mathbf{I}(0)$. For the smallest

(largest) $\mathbf{I}(0)$, the best accuracy occurred at the 18-th (14-th) order, showing the asymptotic character of the expansion. On the slower IBM 3090 our calculations for one torus with $M = 10, 20, 30$ took only $3, 28, 126$ seconds, respectively, requiring $3086, 8711, 45398$ map evaluations to find the required orbit points. These times are not directly comparable to times for the method of Ref. 8 , since the latter produces a full canonical transformation, not just a single torus. It has been shown that a few tori, interpolated in $\mathbf{J}$, can produce equivalent information.[11]

It appears from these results on a nontrivial and fairly typical example that the method promises real progress in the long standing effort to compute invariant tori.

I wish to thank R.Ruth, É. Forest, J. Irwin, and J. S. Berg for their generous interest in this work and valuable suggestions.

References

1. G. Gallavotti, *The Elements of Mechanics*, (Springer, New York, 1983).
2. A. H. Reiman and N. Pomphrey, *J. Comp. Phys.*, in press.
3. C. C. Martens and G. S. Ezra, J. Chem. Phys. **86**, 279 (1987).
4. J. Binney and D. Spergel, Astrophys. J. **252**, 308 (1982).
5. R. D. Ruth, *Physics of Particle Accelerators, Vol. 1, AIP Conf. Proc.* **153**, (Amer. Inst. Phys., New York, 1987).
6. H. Poincaré, *Les Méthodes Nouvelles de la Mécanique Céleste, Vol. 1*, (Gauthier-Villars, Paris, 1892).
7. A. Deprit, Cel. Mech. **1**, 12 (1969).
8. É. Forest, M. Berz, and J. Irwin, Part. Accel. **24**, 91 (1989).
9. R. L. Warnock and R. D. Ruth, Physica **26D**, 1 (1987).
10. W. E. Gabella, R. D. Ruth, and R. L. Warnock, *Proc. 1989 IEEE Part. Accel. Conf., Chicago, March 20–23, 1989*, eds. F. Bennett and J. Kopta (IEEE, New York, 1989).
11. R. L. Warnock and R. D. Ruth, Phys. Rev. Lett. **66**, 990 (1991); SLAC–PUB–5304, 1990, to be published in *Proc Workshop on Nonlinear Problems in Future Particle Accelerators*, Capri, Italy, April 19–25, 1990, ed. G. Turchetti, (World Scientific, Singapore).
12. N. N. Nekhoroshev, Russian Math. Surveys **32**:6, 1 (1977).
13. É. Forest and R. D. Ruth, Physica **43D**, 105 (1990).
14. M. Hénon and C. Heiles, Astron. J. **69**, 73 (1964).

Table Caption

TABLE 1.

Relative deviations of orbits from tori after 1000 turns, for an ensemble of 100 orbits. The tori were obtained by fitting orbits with initial action $\mathbf{I}(0)$ and initial angle $\mathbf{\Phi}(0) = 0$ to Fourier series with maximum mode number $M = M_1 = M_2$. The f_i are fluctuations of I_i on the tori.

M	$\max \lvert dI_1 \rvert / J_1$	$\max \lvert dI_2 \rvert / J_2$	$\langle dI_1 \rangle / J_1$	$\langle dI_2 \rangle / J_2$
$\mathbf{I}(0) = (100, 50) \cdot 10^{-8}$ m			$(f_1, f_2) = (0.10, 0.11)$	
30	$1.3 \cdot 10^{-10}$	$1.7 \cdot 10^{-9}$	$1.0 \cdot 10^{-12}$	$1.7 \cdot 10^{-12}$
20	$1.8 \cdot 10^{-9}$	$3.8 \cdot 10^{-9}$	$1.5 \cdot 10^{-11}$	$-9.6 \cdot 10^{-11}$
10	$2.6 \cdot 10^{-5}$	$3.2 \cdot 10^{-5}$	$-7.7 \cdot 10^{-8}$	$1.3 \cdot 10^{-6}$
$\mathbf{I}(0) = (315, 150) \cdot 10^{-8}$ m			$(f_1, f_2) = (0.19, 0.20)$	
30	$3.2 \cdot 10^{-8}$	$1.9 \cdot 10^{-7}$	$5.9 \cdot 10^{-10}$	$1.5 \cdot 10^{-9}$
20	$1.3 \cdot 10^{-7}$	$4.2 \cdot 10^{-7}$	$4.5 \cdot 10^{-9}$	$1.8 \cdot 10^{-9}$
10	$1.9 \cdot 10^{-4}$	$5.6 \cdot 10^{-4}$	$-9.6 \cdot 10^{-7}$	$7.3 \cdot 10^{-6}$
$\mathbf{I}(0) = (630, 305) \cdot 10^{-8}$ m			$(f_1, f_2) = (0.27, 0.31)$	
30	$5.9 \cdot 10^{-6}$	$1.9 \cdot 10^{-5}$	$-4.6 \cdot 10^{-8}$	$1.7 \cdot 10^{-7}$
20	$1.6 \cdot 10^{-4}$	$4.3 \cdot 10^{-4}$	$-4.5 \cdot 10^{-6}$	$-7.0 \cdot 10^{-6}$
10	$9.1 \cdot 10^{-3}$	$2.0 \cdot 10^{-2}$	$8.2 \cdot 10^{-5}$	$7.9 \cdot 10^{-5}$

Figure Captions

Figure 1. Angle coordinates (Φ_1, Φ_2) at $\theta = 0$ for a low-order resonant orbit.

Figure 2. Angle coordinates (Φ_1, Φ_2) at $\theta = 0$ for an apparent nonresonant orbit.

Figure 3. Orbit data at $\theta = 0$ for an orbit with initial conditions $\mathbf{I}(0) = (315, 150) \cdot 10^{-8}$ m, $\mathbf{\Phi}(0) = 0$.

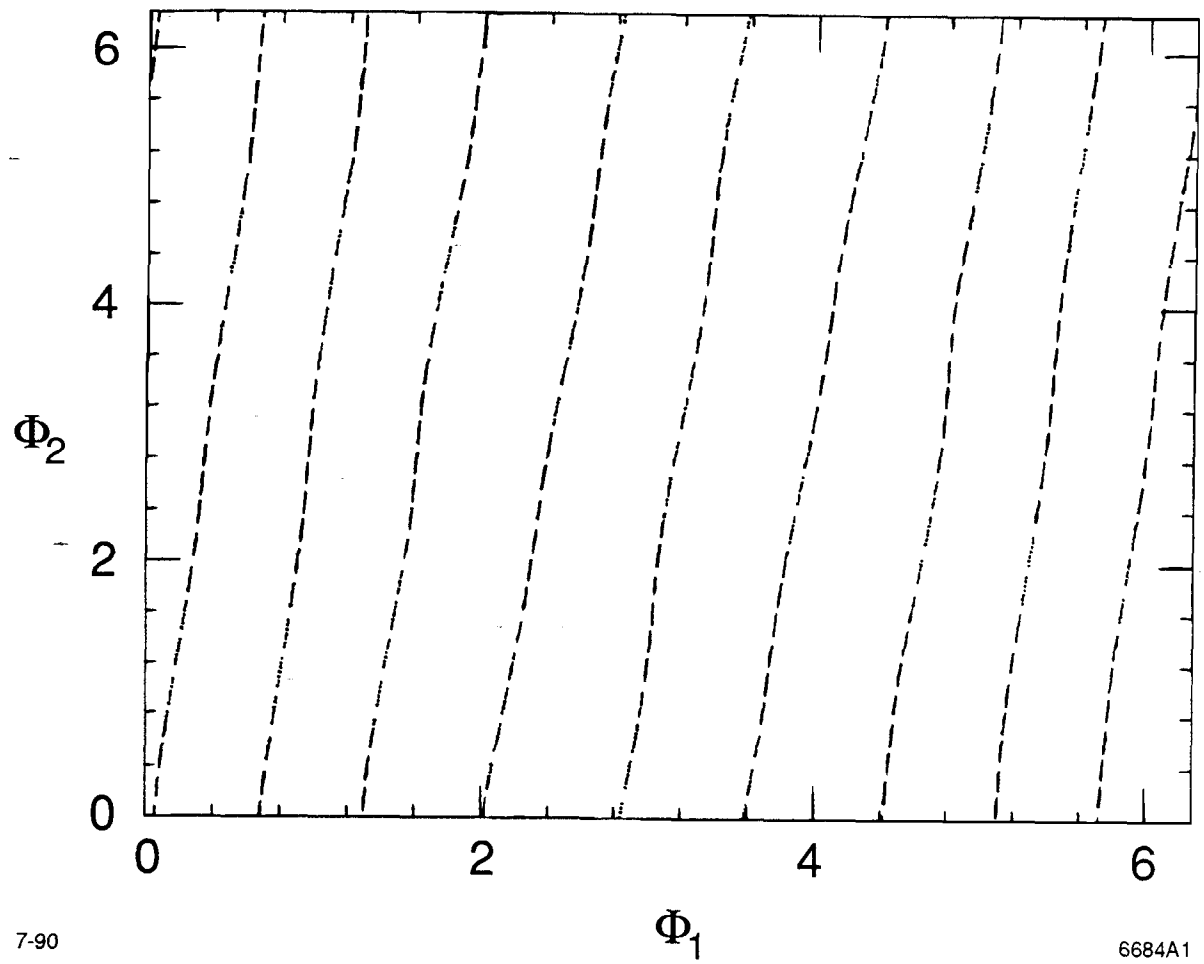

Fig. 1

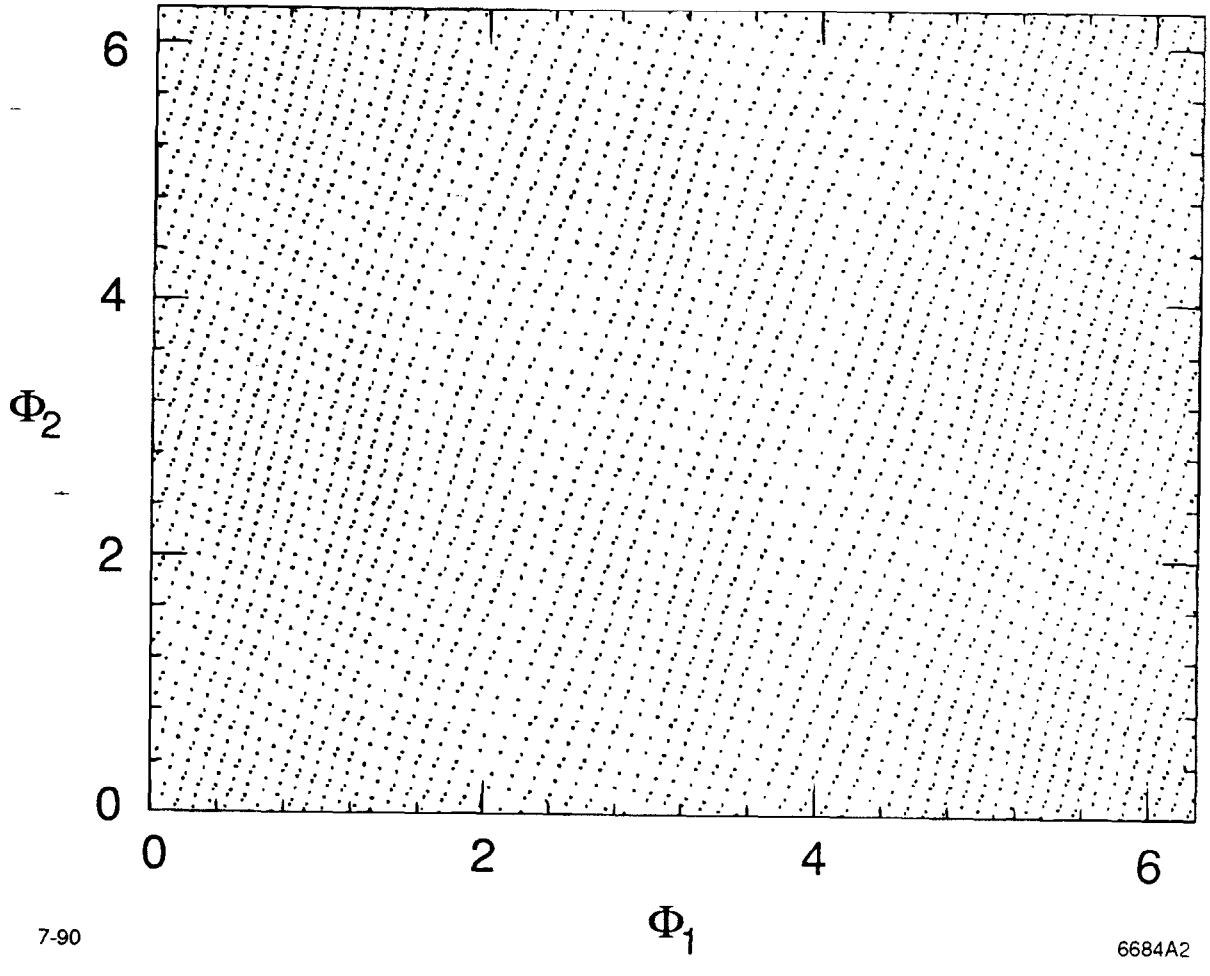

Fig. 2

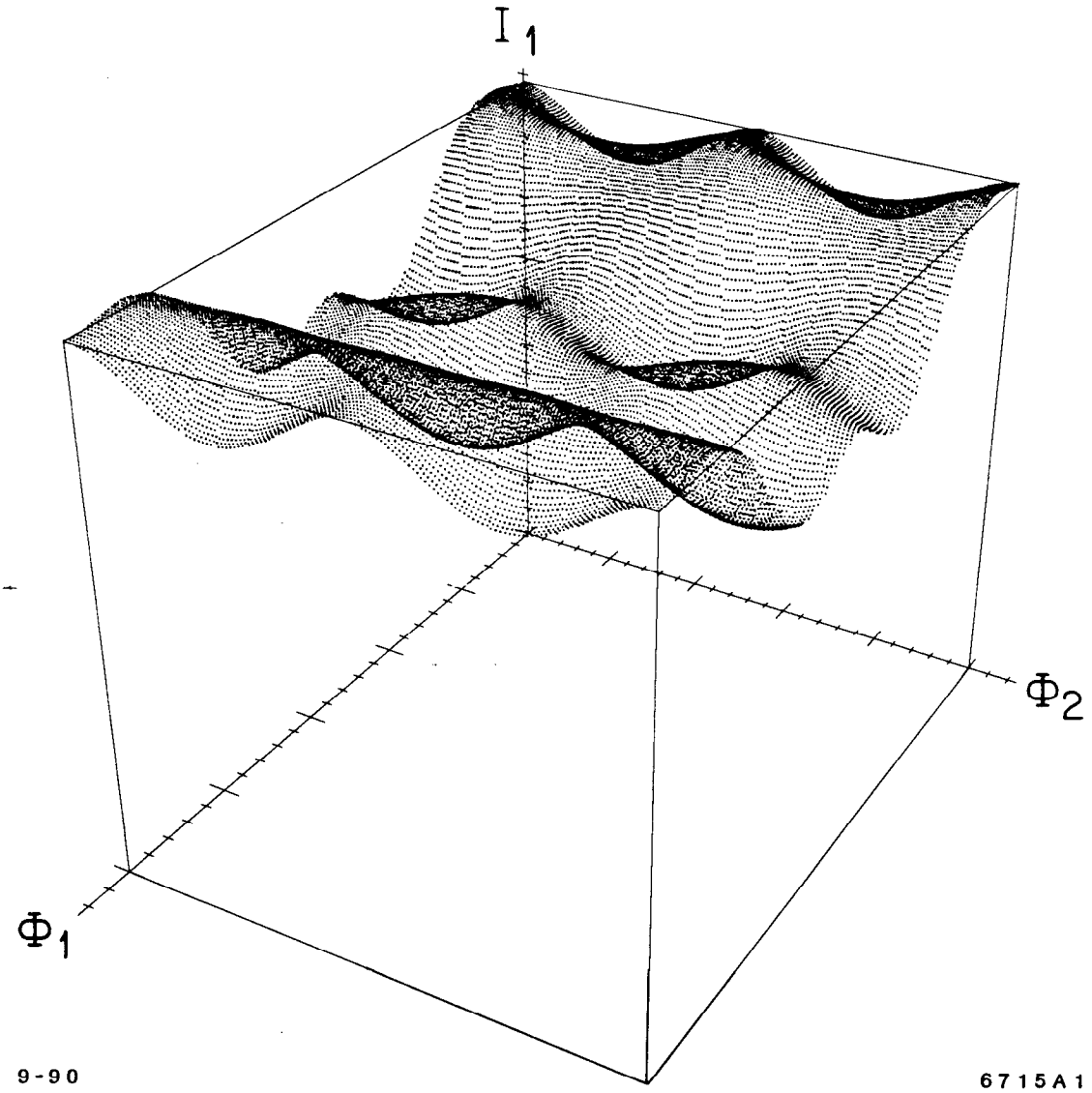

Fig. 3